BASIC PROPERTIES OF STARS. II: SPECTRAL CLASSIFICATION AND THE H-R DIAGRAM

3.1 Introduction

Although the broad spectral distribution of stars approximates that of a blackbody, on closer scrutiny there are deviations (see Figure 2.7). Thus a star colour is not a very precise measure of its temperature. Furthermore, the presence of interstellar dust grains between a star and our telescopes on Earth can extinguish and redden the light (dust grain absorb and scatter photons of shorter wavelengths more readily than those of longer wavelengths). This selective extinction, unless corrected for, can lead us to underestimate the effective temperature of a star.

For all of these reasons, stellar effective temperatures are more accurately determined by measuring discrete spectral features—generally absorption lines—in medium and high resolution spectra of the stars of interest. This is achieved by recording the entire spectrum, normally at optical and infrared wavelengths, of a star with a spectrograph[1] mounted at the focus of a telescope. The move from imaging through just two filters to spectroscopy is time consuming, especially if we are interested in recording the spectra of many stars—within a cluster for example, but the accuracy of the results makes it worthwhile. Indeed, most of what we know about the physical properties of the Universe is derived from the study of spectra of astronomical objects.

We shall return in later lectures to the physical properties of stellar spectra; for the moment we shall limit ourselves to the most important points. The first point to understand is how spectral features are formed, as illustrated in Figure 3.1.

Hot dense objects such as the interiors of stars radiate according to eqs. 2.9 and 2.10. If we were able to view the light from such sources directly,

[1] An instrument which includes light-dispersing elements such as prisms or ruled gratings.

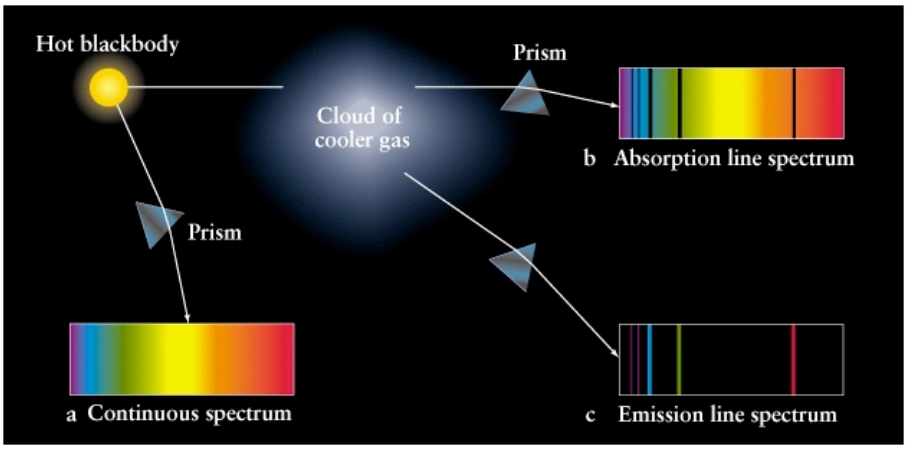

Figure 3.1: Continuum, absorption, and emission spectra of astronomical sources.

without any intervening matter, then the resultant spectrum would appear as a continuum.

Most stars are surrounded by outer layers of gas that are less dense than the core. The photons emitted from the core cover all frequencies (and energies). Photons of specific frequency can be absorbed by electrons in the diffuse outer layer of gas, causing the electron to change energy levels. Eventually the electron will de-excite and jump down to a lower energy level, emitting a new photon of specific frequency. However, the direction of this re-emission is random, so the chance of the re-emitted photon travelling along the same path as the original incident photon is very small. The net effect is that the intensity of light at the wavelength of that photon will be less in the direction of an observer and the resultant spectrum will show dark *absorption* lines. Stellar spectra typically look like this. A digital version of the spectrum, which is just a plot of relative intensity as a function of wavelength, will show reduced intensities—or absorption lines—at specific wavelengths (see, for example, Figure 2.6).

A third possibility occurs if an observer is not looking directly at a hot black body source but instead at a diffuse cloud of gas. If this cloud can be excited by a nearby source of energy, such as hot, young stars or an active galactic nucleus, then the electrons in atoms of the gas cloud can get excited. When they de-excite they emit photons of specific frequency and wavelength. As these photons can re emitted in any direction an external observer will detect light at these wavelengths. The spectrum formed is an *emission* line spectrum. A typical example is the spectrum produced

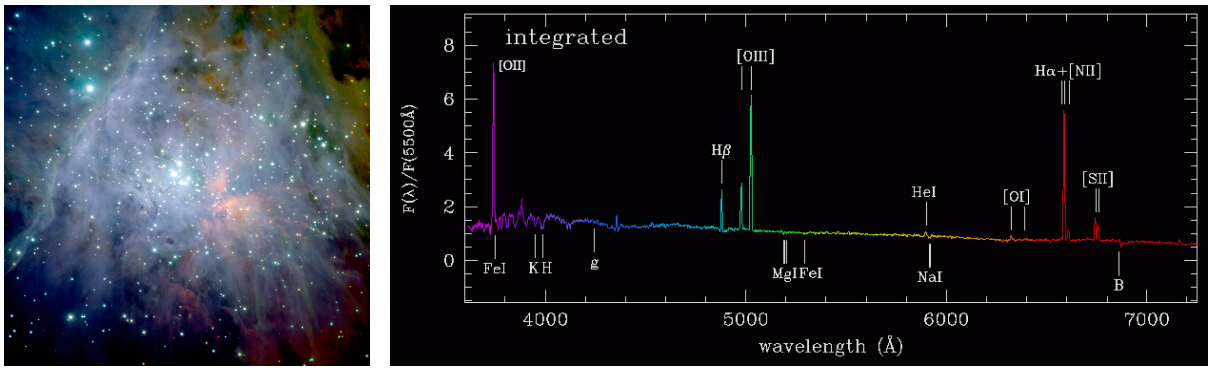

Figure 3.2: Left: Near-IR image of the central part of the Orion nebula, obtained with the ESO VLT. The nebula is diffuse gas ionised by hot stars: the famous Trapezium stars can be seen near the centre together with the associated cluster of about 1,000 stars, approximately one million years old. Right: Typical emission line spectrum of an H II region such as the Orion Nebula. The most important spectral features are labelled.

by the Orion Nebula, our nearest ionised hydrogen, or H II, region (see Figure 3.2.

3.2 Collisional excitation and ionisation

Thermal excitation of different atomic levels and different ionisation stages of the same element becomes significant when the thermal energy kT is comparable to, respectively, the energy difference between different atomic levels and the ionisation potential (binding energy of the electron) of a given ion. For example, in H, with an ionisation potential $\xi_i = 13.6\,\mathrm{eV}$ (see Figure 3.3), this occurs at $T \simeq 10^5\,\mathrm{K}$. At lower temperatures, ionisation or excitation will be incomplete, and the gas will contain a mixture of states.

Referring to Figure 3.3, the number of atoms in an atomic level n with energy E_n is given by the Boltzmann's equation:

$$N_n = A\, e^{-E_n/kT}\, g_n\,, \tag{3.1}$$

where k is Boltzmann's constant ($k = 8.62\times10^{-5}\,\mathrm{eV\,deg^{-1}}$), A is a constant of proportionality and g_n is the statistical weight of atomic level n denoting the number of particles which can be in atomic state n. If J_n is the angular momentum of a state, its electronic statistical weight is $g_n = 2J_n + 1$. The relative populations of two levels of the same atom are therefore:

$$\frac{N_n}{N_m} = \frac{g_n}{g_m}\, e^{-(E_n - E_m)/kT}\,, \tag{3.2}$$

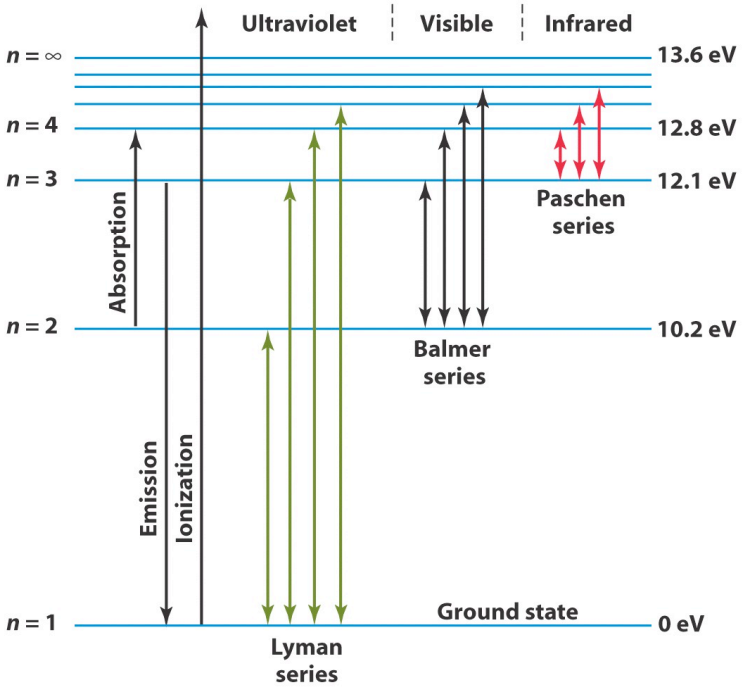

Figure 3.3: Energy levels of the neutral hydrogen atom.

and the total number of atoms in all levels is:

$$N = \sum_{n=1}^{\infty} N_n = A \sum_{n=1}^{\infty} g_n \, e^{-E_n/kT} = A \, Z(T) \,, \tag{3.3}$$

where $Z(T) = \sum_n g_n \, e^{-E_n/kT}$ is the *partition function*.

Eqs. 3.1 and 3.2 have immediate applications to stellar spectra. Consider for example the Hα absorption line which occurs when an electron absorbs a photon with energy $E = h\nu = E_3 - E_2 \simeq 12.09 - 10.20 = 1.89\,\mathrm{eV}$, corresponding to a wavelength $\lambda = 6563\,\text{Å}$ (Figure 3.3). This transition will be strong in the spectrum of a star only if there is an appreciable number of H atoms in the $n = 2$ level capable of absorbing an Hα photon. In other words, we must not have $kT \ll E_2$. With $E_2 = 10.20\,\mathrm{eV}$, we have $T \simeq 1.2 \times 10^5\,\mathrm{K}$. This temperature is much higher than $T_{\rm eff} = 5770\,\mathrm{K}$ of the Sun, which explains why the Hα absorption line is not very strong in the Sun. Its strength in stars increases in stars hotter than the Sun, and peaks in stars with $T_{\rm eff} \simeq 10\,000\,\mathrm{K}$ (such as α Lyr; see Table 2.2).

In stars with $T_{\rm eff} > 10\,000\,\mathrm{K}$, the strength of H$\alpha$ decreases again, because of the increasing fraction of H that is ionised, due to collisional ionisation. The relative proportions of ions in two successive stages of ionisation is

given by the Saha equation:

$$\frac{n_e \cdot N_{i+1}}{N_i} = 2\,\frac{Z_{i+1}}{Z_i}\,\frac{(2\pi m_e kT)^{3/2}}{h^3}\,e^{-\chi_i/kT} \tag{3.4}$$

which can be derived from consideration of the statistical properties of electrons in the continuum of energy levels. Here, Z_i is the partition function of the ith ionisation stage, χ_i is the ionisation potential of the ith ionisation stage (the energy required to ionise ion i to ion $i+1$), and the other symbols have their usual meaning. Another form of the Saha equation is obtained by multiplying both sides by kT and using the definition of electron pressure $P_e = n_e kT$ to get:

$$\frac{N_{i+1}}{N_i} = 2\,\frac{Z_{i+1}}{Z_i}\,\frac{(2\pi m_e)^{3/2}}{h^3}\,\frac{(kT)^{5/3}}{P_e}\,e^{-\chi_i/kT}\,. \tag{3.5}$$

Trivially, the Saha equation tells us that atoms with low ionisation potentials will be relatively more ionised at any given temperature than atoms of higher ionisation potentials. For the common chemical elements, He and Ne are the hardest to ionise ($\chi_0 > 20\,\mathrm{eV}$), H, C, N, O are the next ($20\,\mathrm{eV} > \chi_0 > 10\,\mathrm{eV}$), and the easiest are Li, Na, Mg, Al, Ca with $\chi_0 \sim 5\,\mathrm{eV}$. Because χ_0 appears in the exponential in the Saha equation, this difference has a profound effect in the relative abundances of different ions. For example, $N(\mathrm{Na}^+) \propto e^{-5.16\,\mathrm{eV}/kT}$, while $N(\mathrm{H}^+) \propto e^{-13.6\,\mathrm{eV}/kT}$. Thus, in the Sun ($T = 5770\,\mathrm{K}$), $N(\mathrm{Na}^+)/N(\mathrm{Na}) \sim 10^7 N(\mathrm{H}^+)/N(\mathrm{H})$.

This difference more than makes up the low ratio $N(\mathrm{Na})/N(\mathrm{H}) \sim 10^{-6}$ in the Sun. Thus, in the solar atmosphere, the free electrons present are predominantly from atoms of low ionisation potential, such as Na, Ca, Al, and so on. These free electrons, from the metals, have an impact on the degree of ionisation of H through the n_e term in the Saha equation. The corollary of this statement is that variations in metal abundances from one star to another may have a major effect on the physical state of the gas, especially its ionisation equilibrium.

Returning to our main point, it is now easy to see that by considering the relative strengths of absorption lines of elements in different ionisation and excitation states, it is possible to deduce the effective temperature of the stellar atmosphere. Hotter stars will have absorption lines from highly ionised stages, while the coolest stars can even maintain significant densities of molecules in their atmospheres—see Figure 3.4.

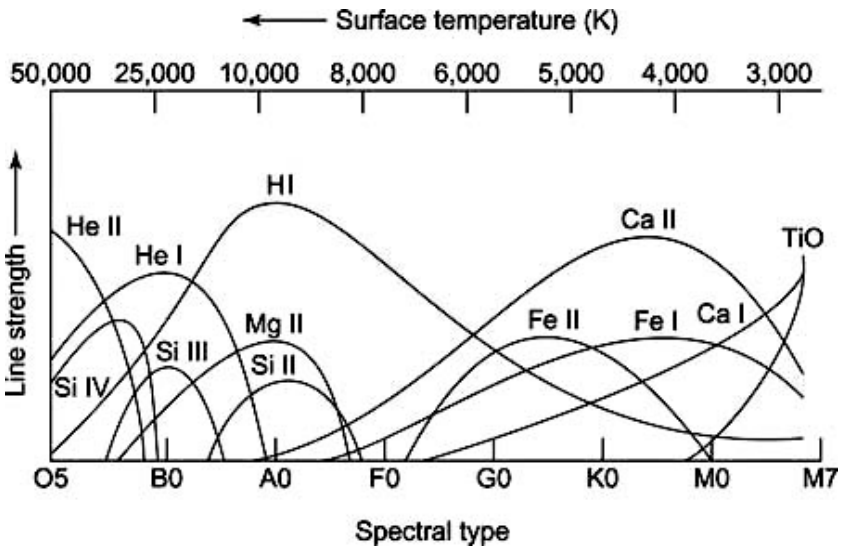

Figure 3.4: Dominant ions in stars of different effective temperatures.

3.3 Stellar Spectral Types

The classification of stellar spectra originates from a time (late 1800s–early 1900s) when their physical meaning was not understood. The Harvard classification scheme is a one-dimensional scheme which divides stars into a sequence of seven classes, O, B, A, F, G, K, M, based on their effective temperature, as follows:

Class	$T_{\rm eff}$ (K)
O	$\geq 33\,000$
B	$10\,000 - 33\,000$
A	$7500 - 10\,000$
F	$6000 - 7500$
G	$5200 - 6000$
K	$3700 - 5200$
M	≤ 3700

Typical spectra for stars of different classes are shown in Figure 3.5. Each class is subdivided into 10 sub-classes, with $T_{\rm eff}$ decreasing from sub-class 0 to 9. Thus we have spectral classes O9 and B0, the former being just hotter than the latter. Division between subclasses can be finer, e.g. class O9.5. O and B stars are sometimes referred to as 'early-type', while K and M are 'late-type'.

The Sun has spectral class G2. More recently the classification has been

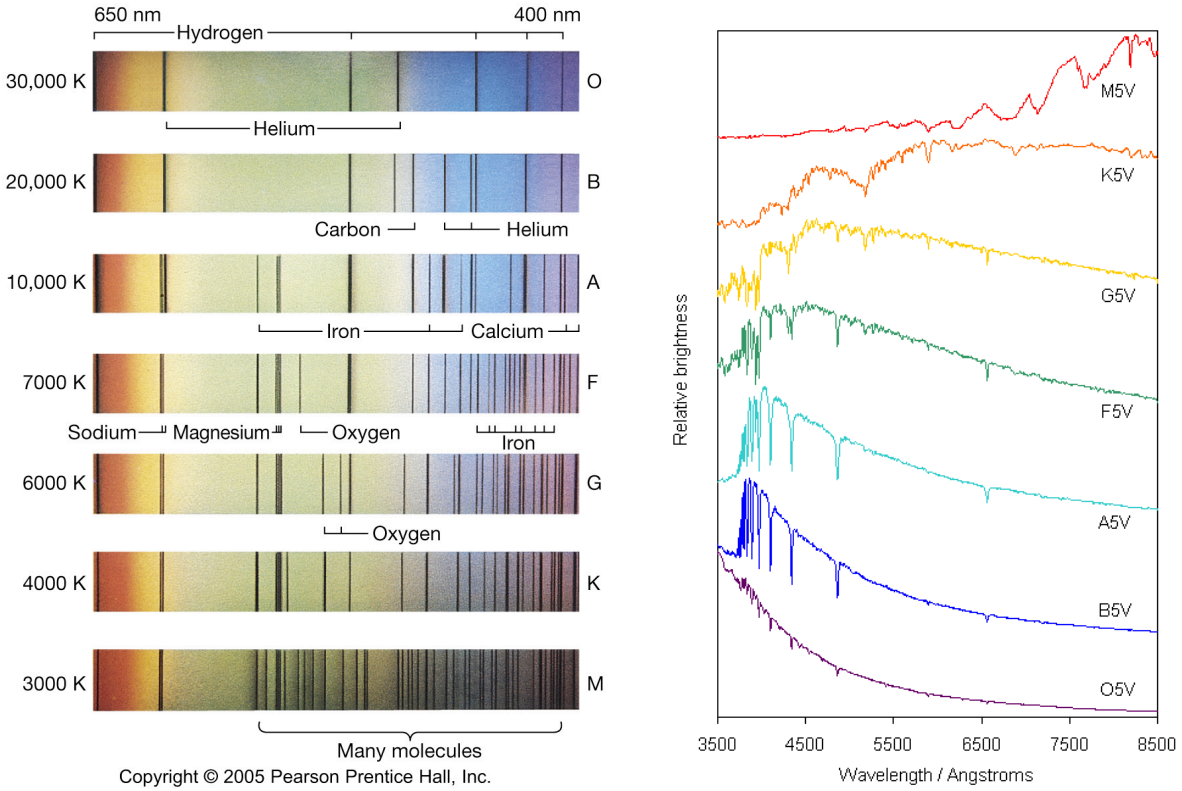

Figure 3.5: Typical spectra of different stellar spectral classes .

extended to cooler stars, so cool that they are brightest at infrared wavelengths, with classes L and T (mostly brown dwarfs which do not achieve sufficiently high temperatures in their cores to ignite thermonuclear fusion).

3.4 Luminosity Classes

As we shall study in more detail later in the course, the spectra of stars give a great deal more information on their physical properties than just a measure of $T_{\rm eff}$. For our present purposes all we have to appreciate is that the *profile*, as well as the overall strength, of an absorption line gives information about conditions in the gas that produced it. In particular, the width of an absorption line depends on the density of the stellar atmosphere where it was formed. If we consider stars of the same $T_{\rm eff}$ but different radii, the surface density and gravity are lower in stars of larger radii. As a consequence, more luminous stars (at a given $T_{\rm eff}$, recall eq. 2.15) have narrower absorption lines. Thus, the absorption line widths provide a measure of the 'Luminosity Class'.

Luminosity classes are indicated by roman numerals, from I to V in order

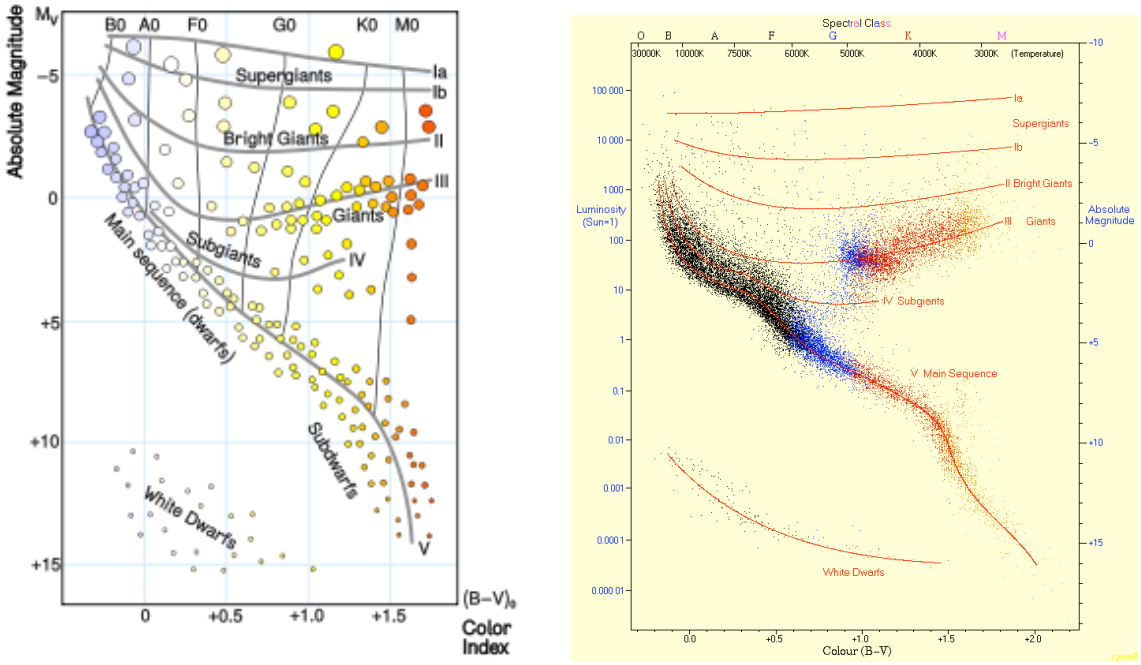

Figure 3.6: Left: Schematic representation of the MK stellar classification scheme. Right: Luminosity classes in the Hipparcos H-R diagram for nearby stars.

of *decreasing* luminosity. Class I is further sub-divided into classes Ia and Ib—these are the *'supergiants'*. Stars of luminosity class III are referred to as *'giants'*. Stars on the main sequence are given luminosity class V and, confusingly, are sometimes referred to as *'dwarfs'*. The luminosity class, together with the spectral class, results in the two-dimensional M-K stellar classification scheme (see Figure 3.6). Table 3.1 now includes the M-K spectral type for the same nearby stars considered in Table 2.2.

Table 3.1 Spectral types, $B-V$ colours and effective temperatures of some nearby stars

Object	Spectral Type	$B-V^{\dagger}$ (mag)	$T_{\rm eff}$ (K)
HD 14434	O5 V	−0.33	47 000
ζ Oph	O9 V	−0.31	34 000
τ Sco	B0 V	−0.30	30 000
α Lyr	A0 V	0.00	9790
51 Aql	F0 V	+0.30	7300
Sun	G2 V	+0.63	5777
31 Ori	K5 III	+1.50	4050
19 Ari	M0 III	+1.56	3690
α Ori	M2 I	+1.71	3370
Wolf 359	M6 V	+2.03	2800

† Corrected for interstellar reddening

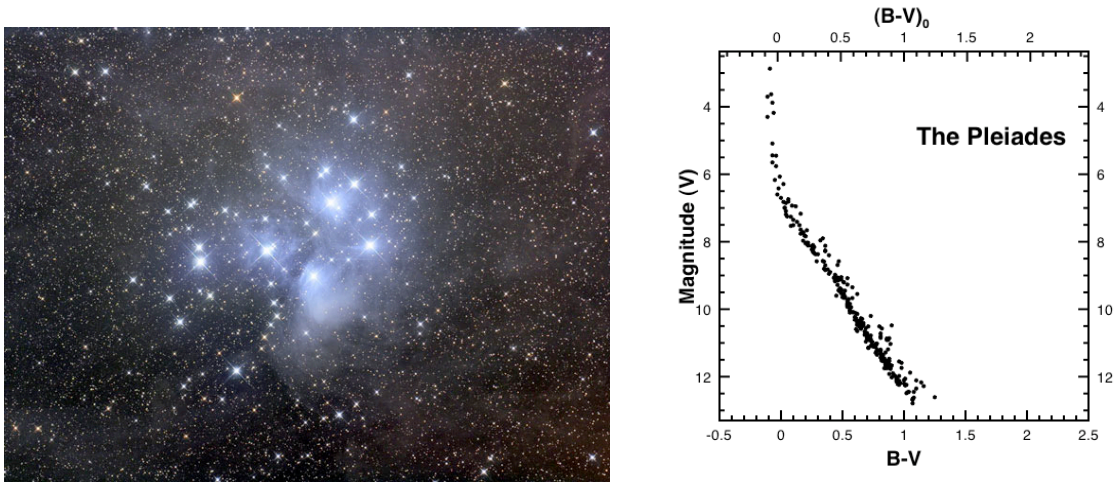

Figure 3.7: The Pleiades: a young star cluster and its colour-magnitude diagram.

3.5 Cluster HR Diagrams

Constructing colour-magnitude diagrams for stellar clusters where all the stars are coeval and have the same chemical composition (since they were presumably born out of the same interstellar cloud) allows us to consider evolutionary effects on the HR diagram.

The Pleiades (Figure 3.7) are a famous stellar cluster visible from northern skies in the winter. At a distance of only 120 pc, it is one of the closest open star cluster. It consists of over 1000 stars, of which the brightest are mid- to late-B type stars. Its colour-magnitude diagram (right panel of Figure 3.7) shows a well populated main sequence up to stars with $(B-V) \simeq 0.0$, corresponding to $T_{\rm eff} \simeq 10\,000\,{\rm K}$. The earliest main sequence star in the Pleiades is of spectral type B8V (18 Tau). The absence of hotter stars in the colour-magnitude diagram indicates an age of $\sim 10^8$ years; hotter and more massive stars evolve off the main sequence in less than 10^8 years.

Contrast Figure 3.7 with Figure 3.8, an old globular cluster in the halo of the Milky Way. At a distance of 10 kpc from the Sun, M3 contains approximately half a million stars. Its age is estimated to be $\sim 8 \times 10^9$ years from the fact that only relatively cool stars, with $(B-V) \simeq +0.4$ (late F) are found on the main sequence.

The right panel of Figure 3.8 illustrates the nomenclature applied to different regions of the HR diagrams, in accordance with our understanding of the stages they represent in the evolution of a star. Anticipating the material to be considered in future lectures, I briefly describe them here.

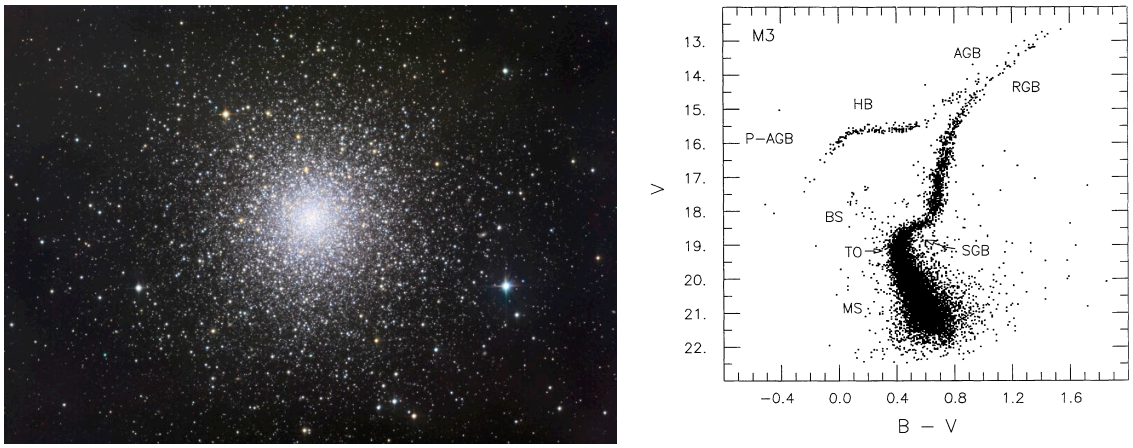

Figure 3.8: M3: an old halo globular cluster and its colour-magnitude diagram.

In the case of a halo globular cluster, with little foreground contamination, the density of points in the HR diagram approximately reflects the length of time a star spends in different evolutionary stages. Stars spend most of their lives on the main sequence (MS), burning hydrogen in their cores. Then turn-off point (TO) marks the end of the MS phase. The lifetime of the most massive star still on the MS then defines the age of the cluster. The TO point is the start of the subgiant branch (SBG) with shell H burning; the star increases in brightness and evolves to the red giant branch (RGB). Here the star loses mass and eventually becomes a horizontal branch (HB) star. The final evolution of the star may lead up to the asymptotic giant branch (AGB) and into the very hot post-asymptotic giant branch (P-AGB). Blue stragglers (BS) are thought to be stars that have been severely affected by close encounters in the dense cluster region or by mass transfer in binary systems.

Thus, a star of a given mass travels through a well specified path, or track, in the colour-magnitude diagram during its lifetime, from its birth to its death, be it a supernova or a cooling white dwarf.

On the other hand, an isochrone is a line on the CMD which defines all stars of a given age. Fitting theoretical isochrones, computed according to stellar evolution theory, to accurate photometry of globular cluster stars gives us estimates of the cluster ages (see Figure 3.9). For a long time, there was a conflict between the ages of the oldest Galactic globular clusters so deduced and estimates of the age of the Universe based on the favoured values of the Hubble constant and of the matter density $\Omega_{\mathrm{M},0}$. This conflict has now been largely resolved: the age of the Universe in today's consensus

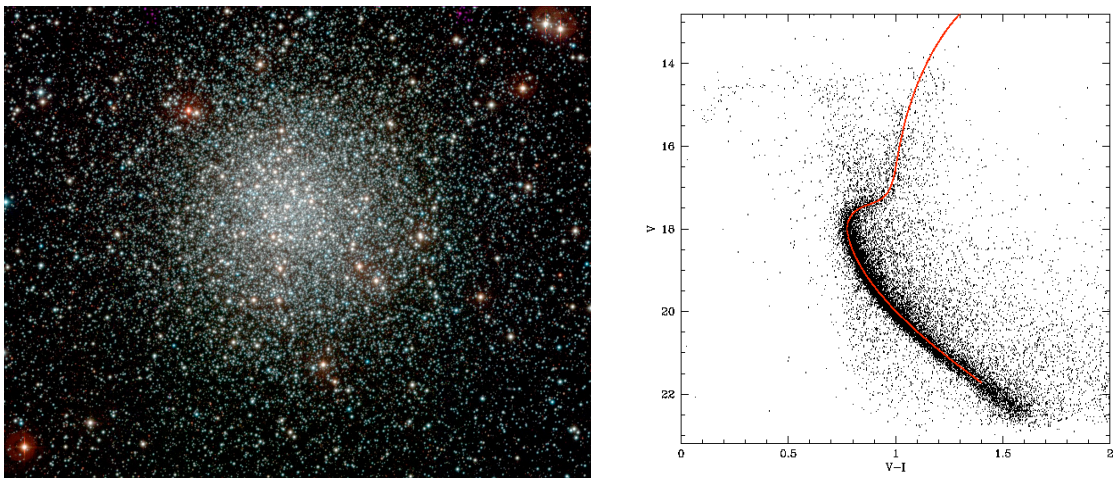

Figure 3.9: NGC 3201, a low Galactic latitude globular cluster at a distance of 5.2 kpc from the Sun. This globular cluster has a relatively low concentration of stars near its center. By fitting its reddening-corrected colour-magnitude diagram with a theoretical isochrone appropriate to its low metallicity ($[\mathrm{Fe/H}] = -1.54$), a best fitting age $t = 12\,\mathrm{Gyr}$ is deduced (von Braun & Mateo 2001, AJ, 121, 1522).

cosmology, $t = 13.7\,\mathrm{Gyr}$, is 'comfortably' greater than the age $t = 12.4\,\mathrm{Gyr}$ of the oldest globular clusters of the Milky Way.

Isochrone fitting to colour-magnitude diagrams is a powerful way to unravel the past history of star formation in a galaxy, as it can reveal distinct episodes of star formation, particularly if they were separated by quiescent periods. Figure 3.10 shows an example for a rich star cluster in our neighbouring galaxy, the Large Magellanic Cloud.

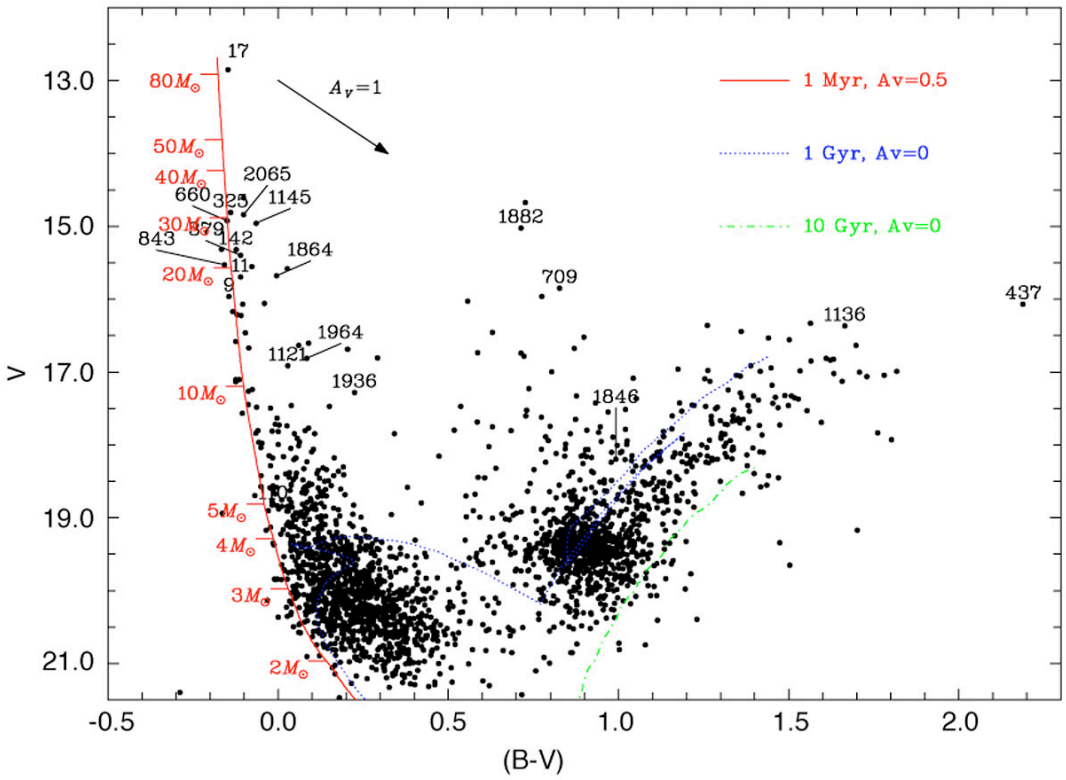

Figure 3.10: Colour-magnitude diagram of 2341 stars observed in the cluster N214C of the Large Magellanic Cloud. Three theoretical isochrones are shown, representing the positions of stars with ages of 1×10^6 years (red curve), 1×10^9 years (dotted blue), and 1×10^{10} years (dashed-dotted green), computed for the LMC metallicity and distance. It is clear from this diagram that N214C is composed of two populations: a very young one, containing very massive stars, and an older one. Star numbered 17 is of spectral type O2 V, one of only a handful of stars known with such an early spectral type. (Figure reproduced from Meynadier et al. 2005, A&A, 436, 117).